

RECENT RESULTS OF SUPER-KAMIOKANDE

Yusuke Koshio

Kamioka observatory, ICRR, University of Tokyo, Hida, 506-1205, Japan

Abstract

The recent results of atmospheric and solar neutrino measurements in the first (SK-I) and second (SK-II) phase of Super-Kamiokande were presented. The neutrino oscillation analysis in atmospheric neutrino was discussed. The best-fit parameters of $(\Delta m^2, \sin^2 2\theta) = (2.5 \times 10^{-3} \text{ eV}^2, 1.0)$ which was combined in SK-I and SK-II were obtained with $\nu_\mu \leftrightarrow \nu_\tau$ two-flavor oscillation model using zenith angle analysis. Other hypotheses to explain the atmospheric neutrino data were not well supported using L/E analysis method. The three-flavor oscillation analysis was also applied. No significant enhancement due to matter effect, which occurs when neutrinos propagate inside the Earth on the condition of $\theta_{13} \neq 0$, cannot be seen. The results of solar neutrino data from SK-I and SK-II were presented. Super-Kamiokande can measure not only the solar neutrino flux but also its energy spectrum and time variations such as day-night and seasonal differences. The detail oscillation analysis using those information are applied to SK-I data. Combining SK and SNO data, the obtained oscillation parameters becomes so-called 'LMA' solution. And also three-flavor oscillation analysis was applied to solar neutrino data, the upper limit for $\sin^2 \theta_{13}$ is 0.067 at 90%C.L..

1 Status of Super-Kamiokande

Super-Kamiokande (SK) is a 50000 ton imaging water Cherenkov detector in the Kamioka mine in Gifu Prefecture, Japan. Cherenkov light generated by charged particles scattered by neutrinos in water are detected by 20-inch photomultiplier tube (PMT). The SK-I started from 1996 and ended to 2001, which live time is 1489 days for atmospheric neutrino and 1496 days for solar neutrino analysis, with 11146 PMTs. The SK-II has started since 2002 with 5182 PMTs, which are covered by acrylic and FRP cases. SK-II phase will be finished 2005. In the paper, the results of SK-II 627 days of data for atmospheric neutrinos (FC/PC data, see the next section), 609 days for upward going muon data, and 622 days for solar neutrinos are presented. After full reconstruction, we will start SK-III with 11146 PMTs from June of 2006.

2 Atmospheric neutrinos

2.1 Detection method

The atmospheric neutrinos are generated via the following process; when primary cosmic rays, such as proton and He, interact with nuclei in the atmosphere of the earth, secondary particles, mostly pions and kaons are produced in the hadronic shower. Atmospheric neutrinos are generated from decay of those secondary particles. The zenith angle, path length and neutrino energies are obtained in Super-Kamiokande atmospheric neutrino analysis, and neutrino oscillation analysis were done using them. The event sample observed in Super-Kamiokande are categorized to three types, fully-contained (FC), partially-contained (PC) and upward-going muons. FC and PC events are generated inside the detector, and the former deposit all of their Cherenkov light in the inner detector, while the latter have exiting tracks and some energy deposit in the outer detector. Upward-going muons are the high energy muons, which are generated in the surrounding rocks and intersect the detector. FC events are divided by their number of Cherenkov rings (single-ring or multi-ring), particle type (e-like or μ -like) and visible energy (sub-GeV or multi-GeV), to infer their original neutrino properties in detail. The events which visible energy is less (greater) than 1.33 GeV are classified as sub-GeV (multi-GeV). Upward-going muons are also divided into two types, (through-going or stopping), according to that the entering muons penetrate or stop inside the detector.

2.2 Results and implication

2.2.1 Zenith angle analysis

The $\nu_\mu \leftrightarrow \nu_\tau$ two-flavor oscillation analysis was carried out using all the atmospheric neutrino data of FC, PC and upward-going muon events. The zenith

angle distribution in each energy region is most powerful method for neutrino oscillation analysis. Fig.1 shows the zenith angle distributions of each samples. The expected distributions with the best fit case of $\nu_\mu \leftrightarrow \nu_\tau$ oscillations well matched to the observed data.

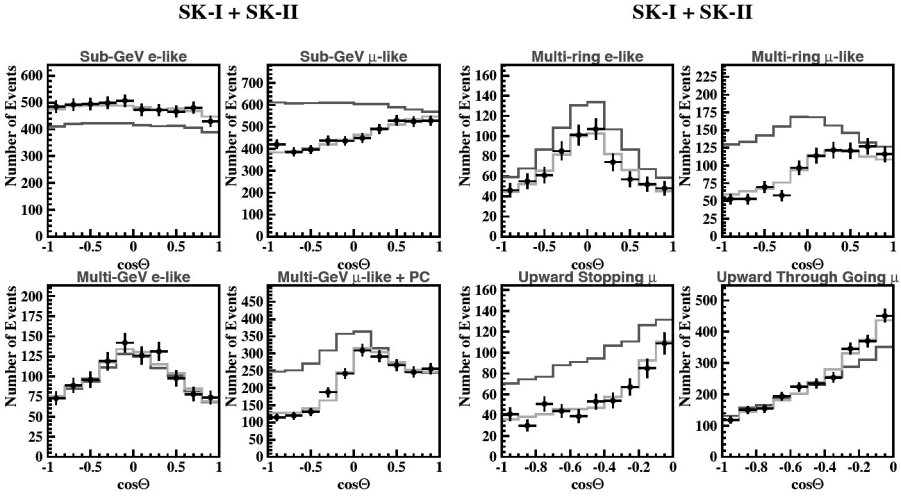


Figure 1: Zenith angle distributions of SK-I and SK-II combined data. Dots with error bars correspond to data. The line along to data shows MC with best fit, and the line away from the data shows MC with no oscillation, respectively.

A χ^2 value between data and expectation was calculated for each set of oscillation parameters. The expected distribution was modified so as to fit the data within the allowable range by the systematic errors, with a constraint to the χ^2 value. Fig.2 shows the allowed region of neutrino oscillation parameters in SK-1 and SK-2 combined. The χ^2 value becomes minimum at $(\Delta m^2, \sin^2 2\theta) = (2.5 \times 10^{-3} \text{ eV}^2, 1.0)$, and parameter region of $0.93 < \sin^2 2\theta$ and $2.1 < \Delta m^2 < 3.0 \times 10^{-3} \text{ eV}^2$ were allowed at 90 % C.L..

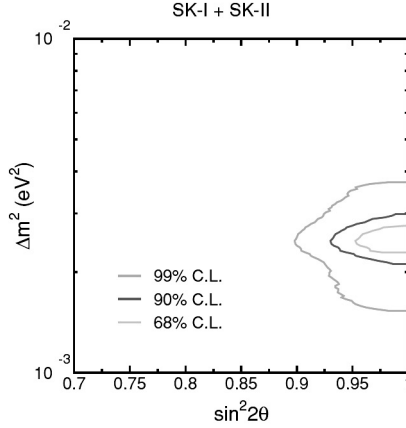


Figure 2: Allowed region of neutrino oscillation parameters in zenith angle analysis of FC, PC and upward going muon in SK-1 and SK-2 combined.

2.2.2 L/E analysis

'L/E' (L means path length and E is neutrino energy) is another powerful tool of neutrino oscillation analysis, since the survival probability in neutrino oscillation is

$$P(\nu_\mu \rightarrow \nu_\mu) = 1 - \sin^2 2\theta \sin^2 \left(\frac{1.27 \Delta m^2 (\text{eV}^2) L (\text{km})}{E (\text{GeV})} \right). \quad (1)$$

If neutrino oscillation is happen, the L/E distribution is expected to appear a clear dip. Therefore, the point of the analysis is seeing this kind of dip and how large it. This analysis is strong constraint on Δm^2 , and possible to check some exotic hypothesis. The left plot in fig. 3 shows the L/E distribution for SK-1 and SK-2 combined data. The data has clear dip around order of 10^2 . There are some models which explain the dip, therefore, the χ^2 differences with $\nu_\mu \leftrightarrow \nu_\tau$ oscillation was calculated in order to validate their reliability. Among three models, neutrino oscillation is most confident. The neutrino decay is 4.4σ away from neutrino oscillation, and the decoherence is 4.8σ away.

The right plot in fig.3 shows the allowed region by L/E analysis in SK-1 and SK-2 combined. The parameter region at 90%C.L. are $0.92 < \sin^2 2\theta$ and $2.0 < \Delta m^2 < 2.9 \times 10^{-3} \text{ eV}^2$.

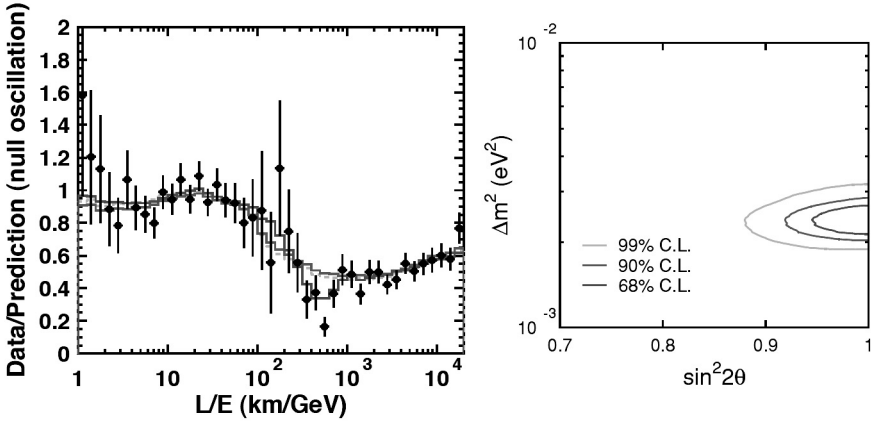


Figure 3: (Left) The ratio between data and prediction as a function of L/E for SK-1 and SK2 combined data. The lines show expectation of several models, neutrino oscillation, neutrino decay and decoherence. (Right) The allowed neutrino oscillation parameter region using L/E analysis.

2.2.3 3 flavor analysis

Though we consider complete neutrino oscillation analysis, the oscillation probabilities can be much simply expressed by Δm_{23}^2 (one mass scale dominance), θ_{23} and θ_{13} , if we assume $|\Delta m_{23}^2| \gg |\Delta m_{12}^2|$ and CP-violation phase is zero. 1, 2) The three-flavor oscillations in the multi-GeV energy range around 1–10 GeV can be drastically changed by matter effect 5) even if θ_{13} is small. The Earth matter effect can resonantly enhance oscillations concerned with electron neutrino, while oscillations for anti-neutrino is suppressed. This effect is expected to be appeared as the marginal excess of upward-going ν_e -rich sample.

As a result of the global scan to the zenith angle distribution on the oscillation parameter grid, the allowed region in each parameters are shown in fig.4. The minimum χ^2 value is obtained at the grid point of $(\Delta m^2, \sin^2 \theta_{23}, \sin^2 \theta_{13}) = (2.5 \times 10^{-3} \text{ eV}^2, 0.5, 0.0)$ for normal hierarchy, and $(2.5 \times 10^{-3} \text{ eV}^2, 0.525, 0.00625)$ for inverted hierarchy, which is consistent with $\nu_\mu \leftrightarrow \nu_\tau$ two-flavor oscillation.

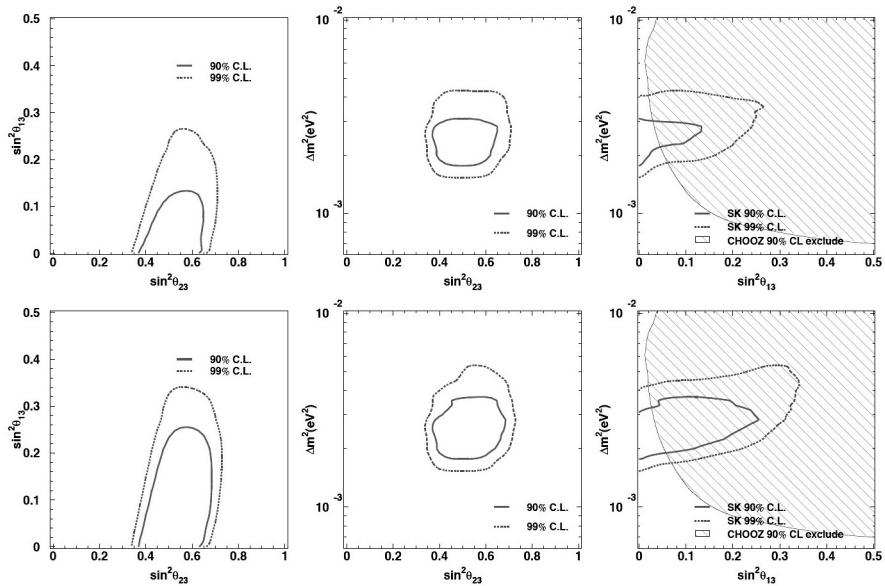


Figure 4: Allowed region for 3 flavor neutrino oscillation analysis using zenith angle distribution in atmospheric samples. Upper shows the normal hierarchy and lower shows the inverted hierarchy case.

3 Solar neutrinos

3.1 Detection method

In Super-Kamiokande, recoil electrons generated by the following elastic scattering process;

$$\nu + e \rightarrow \nu + e \quad (2)$$

were measured. This reaction is preserved the direction of the original neutrinos, so the peak of solar neutrino's direction is clearly found. And the detector can measure not only the solar neutrino flux but its energy spectrum and flux time variation. (day/night or seasonal differences) The energy of recoil electrons are very precisely calibrated ³⁾, it can achieve the very precise neutrino oscillation analysis.

3.2 Results

3.2.1 Solar neutrino flux

The results of observed solar neutrino flux are as follows;

- SK-I (energy threshold is 5.0MeV),

$$2.35 \pm 0.02(stat.) \pm 0.08(sys.) \quad [\times 10^6/cm^2/sec]$$

- SK-II (energy threshold is 7.0MeV),

$$2.36 \pm 0.06(stat.) \quad [\times 10^6/cm^2/sec].$$

Both fluxes between SK-I and SK-II were consistent.

3.2.2 Day-Night flux differences

Day-night flux differences are also measured, and the results were,

$$\frac{D - N}{(D + N)/2} = -0.021 \pm 0.020(stat.)^{+0.013}_{-0.012}(sys.) \quad (SK - 1) \quad (3)$$

$$= -0.014 \pm 0.049(stat.) \quad (SK - 2) \quad (4)$$

The MSW effect ⁵⁾ through the earth, which is ν_e regeneration, could cause flux differences between daytime and night-time. The expected day-night asymmetry assuming 'LMA' solution in the neutrino oscillation is around -1.0% to -1.6%. Both results between SK-I and SK-II are consistent within uncertainties, but they are quite large comparing its expectation. The detection possibility of the day-night asymmetry in the future larger detector may be appeared.

3.2.3 Seasonal variation

In some neutrino oscillation parameters, so-called vacuum oscillation, the distortion of seasonal variation of solar neutrino flux will be appeared. fig.5 shows the solar neutrino flux as a function of time with expectation from the eccentricity of the earth's orbit. The data is very consistent with the expectation.

3.2.4 Spectrum

Fig.6 shows the observed spectrum of recoil electrons observed in SK-I. The vertical axis is normalized by the predicted energy spectrum. We cannot see any distortion.

3.3 Solar neutrino oscillation analysis

3.3.1 In the case of two flavor

For neutrino oscillation analysis, we have introduced the method which is free from the binning of the zenith angle where neutrinos incident to SK detector,

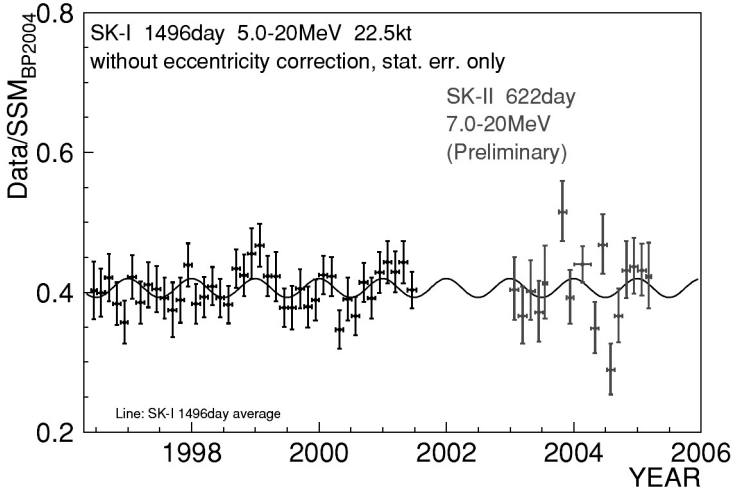


Figure 5: *The time variation of solar neutrino flux in SK-I and SK-II. The solid line shows the expected flux caused by the eccentricity of the earth's orbit.*

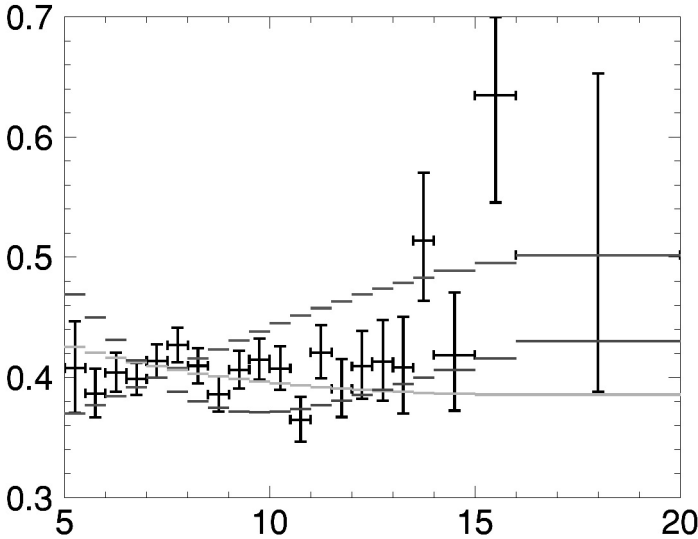


Figure 6: *The spectrum of recoil electron by solar neutrinos in SK-I and SK-II with expected spectrum assuming several neutrino oscillation parameters.*

which means unbinned time variation method. For that purpose, the following Likelihood function is defined on extraction of the solar neutrino signal as

$$L(x) = e^{-(\sigma_i B_i + S)} \prod_{i=1}^{N_{bin}} \prod_{j=1}^{n_i} (B_i u_i(\cos \theta_{sun}) + m_i S p_j(E, \cos \theta_{sun}) \times z_i(t_j)), \quad (5)$$

here B_i is number of backgrounds in each energy bin, u_i is the background shape, S is the number of signals. The last term z_i is the weighting which depends on the event time. Because of this term, it is possible to be free the zenith bins. Fig.7 shows the 95% confidence level excluded and allowed region for neutrino oscillation parameter using SK data. Even only using SK data, large mixing angle region is allowed. And combining SK and SNO data, 'LMA' is the only solution for solar neutrino oscillation.

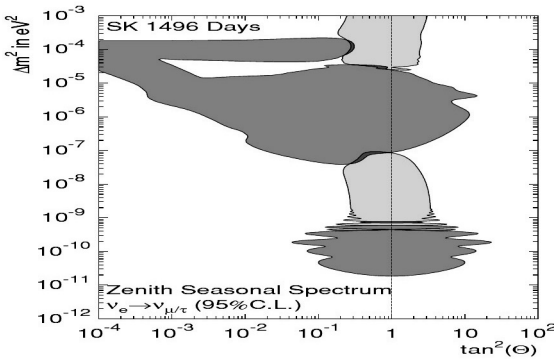


Figure 7: The 95% C.L. excluded and allowed region from SK data.

3.3.2 In the case of three flavor

The ν_e survival probability which go from the sun to the earth is affected by $\sin^2 \theta_{13}$ parameter in 3 flavor neutrino oscillation. And the equation is written using 2 flavor probability as follows;

$$P = (1 - \sin^2 \theta_{13})^2 P^{(2)}((1 - \sin^2 \theta_{13}^2) A(x)) + \sin^4 \theta_{13}, \quad (6)$$

here $P^{(2)}$ shows the survival probability for 2 flavor case. This effect make the matter effect weaken, so the solar neutrino flux, energy distortion and day-night asymmetry is expected to be changed. Using all the solar neutrino data, the $\sin^2 \theta_{13}$ is limited to be less 0.067 at 90% C.L..

4 Summary

In this paper, the recent results of atmospheric and solar neutrino measurements in Super-Kamiokande. For two neutrino oscillation case in atmospheric neutrinos, the two analysis methods, those are zenith angle and L/E analysis is achieved both in SK-1 and SK-2. Both methods make severe constraint to the neutrino oscillation parameters, and also SK-1 and SK-2 results are consistent. In three flavor neutrino oscillation case, it is consistent with $\theta_{13} = 0$ and gives limit to the θ_{13} parameter. In the solar neutrino measurements, SK has precisely observed its flux, recoil electron spectrum and time variations of the flux. No significant time variation and energy distortion appear in SK-1 and SK-2. The solar neutrino oscillation analysis has been done using unbinned time variation method. SK has only large mixing angle region, and combining with SNO, 'LMA' is the unique solution of solar neutrino oscillation.

References

1. G. L. Fogli *et al.*, Phys. Rev. D **55** 4385 (1997)
2. C. Giunti *et al.*, Nucl. Phys. B **521** 3 (1998)
3. M. Nakahata *et al.*, Nucl. Instr. Meth. A421, 113 (1999)
4. J. Bahcall and M.H. Pinsonneault, Phys. Rev. Lett. 92, Number 12, 121301 (2004).
5. S.P. Mikheyev & A.Y. Smirnov, Sov. Jour. Nucl. Phys. 42, 913 (1985),
L. Wolfenstein Phys. Rev. D17, 2369 (1978).